Atmospheric drivers of Antarctic sea ice extent summer minima

Bianca Mezzina[1], Hugues Goosse[1], François Klein[1], Antoine Barthélemy[1], François Massonnet[1]

[1] Earth and Climate Center, Earth and Life Institute, Université catholique de Louvain, Louvain-la-Neuve, Belgium

Correspondence to: Bianca Mezzina (bianca.mezzina@uclouvain.be)

5 **Abstract.** Understanding the variability of Antarctic sea ice is still a challenge. After decades of modest growth, an unprecedented minimum in the sea ice extent (SIE) was registered in summer 2017, and, following years of anomalously low SIE, a new record was established in early 2022. These two memorable minima have received great attention as single cases, but a comprehensive analysis of summer SIE minima is currently lacking. Indeed, other similar events are present in the observational record, although minor compared to the most recent ones, and a full analysis of all summer SIE minima is

10 essential to separate potential common drivers from event-specific dynamics, in order to ultimately improve our understanding of the Antarctic sea ice and climate variability.

In this work, we examine sea ice and atmospheric conditions during and before all summer SIE minima over the satellite period up to 2022. We use observations and reanalysis data and compare our main findings with results from an ocean-sea ice model (NEMO-LIM) driven by prescribed atmospheric fields from ERA5. Examining SIE and sea ice concentration (SIC) anomalies,

15 we find that the main contributors to the summer minima are the Ross and Weddell sectors. However, the two regions play different roles and the variability of the Ross Sea seems to explain most of the minima, with typical negative SIE anomalies about twice the ones in the Weddell Sea. Furthermore, the distribution of SIC anomalies is also different: in the Weddell Sea, they exhibit a dipolar structure, with increased SIC next to the continent and decreased SIC at the sea ice margin, while the Ross Sea displays a more homogenous decrease. We also examine the role of wintertime sea ice conditions before the summer

20 SIE minima and find mixed results depending on the period: the winter conditions seem relevant in the most recent events, after 2017, but marginal for previous years. Next, we consider the influence of the atmosphere on the SIE minima, which appears to play a major role: after analyzing the anomalous atmospheric circulation during the preceding spring, we find that different large-scale anomalies can lead to similar regional prevailing winds that drive the summer minima. Specifically, the SIE minima seem to be associated with dominant north-westerly anomalous winds in the Weddell Sea, while a south-westerly

25 anomalous flow prevails in the Ross Sea. Finally, we investigate the relative contribution of dynamic (e.g. ice transport) and thermodynamic (e.g. local melting) processes to the summer minima. Our results suggest that the exceptional sea ice loss in both the Ross and Weddell sectors is dominated by thermodynamic processes, while dynamics are also present but with a minor role.

1 Introduction

30 Unlike its counterpart in the Northern Hemisphere, Antarctic sea ice extent has started to display signs of a decrease only during the last few years, after a period of overall increase between 1979 and 2016 (e.g. Parkinson and Cavalieri 2012, Hobbs et al. 2016, Parkinson 2019). While it is still unclear whether this is the start of a new trend or just part of the short-term variability, it is certain that the recent period has witnessed some unprecedented events, the latest of which is a new record low of sea ice extent (SIE) in early 2022. After a retreat quicker than usual (Raphael and Handcock, 2022), a record value of 1.92

35 million km^2 was registered on February 25 (Thompson 2022), almost 1 million km^2 below the climatology. This value established a new absolute minimum in the historical record since its predecessor, in 2017, was higher than the symbolic threshold of 2 million km^2 (e.g. Raphael and Handcock, 2022). Even after the growth season and for the rest of 2022, the SIE maintained exceptionally low values throughout the year and has not yet recovered to normal conditions as of early 2023. At the time of submitting this manuscript, it is very likely that 2023 will break a new record low for the February mean sea ice

40 extent.

The February 2022 episode received immediate attention from the scientific community, which did not wait long to provide the first detailed description of the event (Thompson 2022) and preliminary hypotheses on its causes (Raphael and Handcock, 2022). More detailed studies followed shortly after, which investigated the physical drivers and potential mechanisms leading to these extreme conditions. Wang J. et al. (2022) found that the summer SIE minima arose mostly from negative sea ice

45 concentration (SIC) anomalies in the southwestern Amundsen Sea, southeastern Ross Sea, and the northwestern Weddell Sea. They highlighted the contribution of a deepened Amundsen Sea Low (ASL) already during the preceding spring, which was in turn favored by a positive phase of the Southern Annular Mode (SAM). As a result, increased poleward heat transport was found in the Weddell Sea due to anomalous northerly winds on the eastern flank of the ASL, which also pushed more sea ice towards the continent. Concurrently, southerly winds on the western flank of the ASL transported more sea ice towards lower

50 latitudes, favoring melting in the Ross Sea. Furthermore, the authors attributed the negative SIC anomalies to a combination of dynamics and thermodynamics in spring, and to mostly thermodynamic processes in summer. Similar results were obtained by Turner et al. (2022), who further stressed the influence of the anomalously deep ASL on the summer SIC anomalies in the Weddell and Ross seas, but also emphasized the role of a series of intense storms passing in late spring and early summer. More recently, Yadav et al. (2022) specifically focused on the atmospheric precursors of this event during the preceding

55 months, i.e. since September 2021. They highlighted that record SIE values were already registered during the period November-January. Similarly to the other two studies, they also suggested a key role for the ASL, in conjunction with the SAM, during both spring and summer. In addition, they observed a strengthening of the stratospheric polar vortex that could have favored the large-scale tropospheric anomalies.

The previous record minimum in summer 2017 was even more surprising, as it interrupted the modest but robust SIE growing

60 trend of the previous decades (e.g. Zwally et al. 2002; Simmonds et al. 2015; Comiso et al. 2017), which culminated in an all-time maximum in 2014 (e.g. Massonnet et al. 2015). Furthermore, the summer minimum was preceded by a dramatic decrease

already in late spring 2016, which was the focus of most studies (e.g. Turner et al. 2017). This event appeared to be driven by both the ocean and atmosphere (Stuecker et al. 2017; Schlosser et al. 2018; Meehl et al. 2019, Zhang et al. 2022), including the stratosphere (Wang G. et al. 2019), as suggested by observations and climate model simulations (e.g. Kusahara et al 2018;
65 Purich and England, 2019). It resulted from an exceptionally early and rapid ice retreat during the melt season, accompanied by atmospheric circulation anomalies in different sectors, that culminated in November 2016 and continued until March 2017. Similar to 2022, SIE anomalies mainly emerged in the Ross and Weddell Seas, though the spring anomalies were also present in other regions. However, the large-scale atmospheric circulation appeared quite different from the one observed in 2022. In early spring, the atmosphere over the Southern Ocean was dominated by a positive phase of the zonal wave number three
70 (ZW3) pattern, followed by an almost record negative SAM, while the ASL showed no persistent deepening. Additionally, surface and sub-surface ocean conditions played a minor role in driving the minimum itself but contributed to the persistent SIE decline that started in early 2016 (e.g. Zhang et al. 2022).

The 2022 and 2017 minima are widely discussed in the literature as single cases but only a few studies compared them to each other (e.g., Wang et al., 2022) or to other similar events (e.g., Turner et al., 2022). Furthermore, most of these works are based
75 on observations, with limited variables available, and no modelling study for 2022 has been carried out to our knowledge. Unusual anomalous values were also registered during other years and seasons (e.g. Jena et al, 2022) but they received less attention as they did not lead to such extreme absolute SIE. However, analyzing other SIE minima, although minor compared to the recent ones, is essential to further comprehend the dynamics of sea ice variability, the relation between extreme events and atmospheric and ocean conditions, and to potentially interpret the latest records as isolated events or as being part of long-
80 term trends.

In this work, we carry out a comprehensive study of SIE minima over the whole satellite observational period, which is currently lacking. In particular, we focus on summer events, since they typically correspond to absolute yearly minima due to the seasonal cycle of sea ice. It is evident that the two most recent and striking events of 2017 and 2022 present some similarities, such as the regional patterns of SIC anomalies, but are also very different in terms of atmospheric and possibly
85 ocean precursors. Thus, here we compare them to other SIE minima and highlight common features versus event-specific processes. We focus on the atmosphere and examine the large-scale conditions over the Southern Ocean related to the summer SIE minima, but without considering explicitly potential remote drivers and forcings, as in previous works. Instead, we analyze the role of anomalous winds in driving sea ice changes in different regions and the associated processes, and also consider the impact of the previous winter sea ice conditions. In contrast, we do not explore here the contribution from the ocean: while it
90 may have a clear influence on the persistence of the anomalous conditions, it has been shown that its role is minor compared to the atmospheric forcing for the peak of the 2017 and 2022 minima (e.g. Schlosser et al. 2018; Kusahara et al. 2018; Turner et al. 2022; Zhang et al. 2022). This study is based on observations and reanalysis data but also examines results from an ocean-sea ice model driven by observed atmospheric fields.

After presenting the data and methods in Sect. 2, we examine the summer SIE time series and discuss the SIC anomalous
95 patterns during years defined as "minima" (Sect. 3.1 and 3.2) and consider the influence of the sea ice state in the previous

winter (Sect. 3.3). Then, we investigate the atmospheric circulation anomalies during the preceding spring, both at large scale and regionally, by focusing on the prevailing local wind direction (Sect. 3.4). Using a model not only allows us to derive more robust conclusions, but also to further investigate the processes at play thanks to output variables that are not available for the observations. For instance, in Sect. 3.5 we estimate the contribution to anomalous sea ice changes from dynamic and

100 thermodynamic processes by means of online diagnostics in the model. The main findings are summarized and discussed in Sect. 4.

2 Data and methods

2.1 Observations and model

We use observed daily SIC from the EUMETSAT OSI SAF datasets (OSI-450 and OSI-430-b; OSI SAF 2017, Lavergne et

105 al., 2019) and monthly 10-m wind and sea level pressure (SLP) from the ERA5 reanalysis (Hersbach et al., 2020) over the period 1980-2022.

We compare the observations with results from a regional ocean-sea ice model forced by atmospheric conditions from reanalyses over the same period. The ocean model is NEMO3.6 (Madec et al., 2017) coupled to the sea ice model LIM3.6 (Vancoppenolle et al., 2012; Rousset et al., 2015) in a regional configuration that covers the Southern Ocean (SO) from 30° S.

110 The horizontal resolution is close to 1/4° (about 24 km at the 30° S boundary and 14 km at 60° S) and there are 75 vertical levels, with thickness increasing from 1 m at the surface to about 200 m at depth. A full description and evaluation of the model can be found in Pelletier et al. (2022) (specifically, we use the same configuration as in their PAROCE experiment).

In this simulation, ranging from January 1980 to March 2022, the model is driven by atmospheric fields from ERA5 over the SO domain and forced at the ocean boundaries with observations from the ORAS5 oceanic reanalysis (Zuo et al., 2019), while

115 the initial conditions are set using the climatology (1990-2009) from a previous run.

2.2 Methods

We select summer minima common to the model and observations based on January-March (JFM) anomalies of the SIE. We use the standard definition of SIE based on a 15% threshold for SIC. To simplify the selection of the events, we consider the standardized time series by dividing the anomalies by their standard deviation (σ) over the whole period. We first identify

120 circumpolar (hereafter "total") minima using the full SIE computed for the whole SO domain and by selecting those years with anomalies below -1σ in the observations *and* below -0.5σ in the model. With this definition, all the events below -1σ in the observations are selected as minima (Fig. 1a), but we ensure that concurrent substantial negative SIE anomalies occur in the model and are worth exploring further for physical mechanisms (note that considering 1σ also for the model would lead to the selection of only two events). A similar approach is used with the SIE computed only in the Ross sector (160E-130W, see Fig.

125 1f) to identify years that are regional minima, which may not correspond to the ones of the total SIE, as discussed in Sect. 3.1. For the Weddell sector (60W-20E, see Fig. 1f), a slightly different definition is applied due to the smaller SIE variability in

that region (see Fig. 1c). A year is selected as a minimum in the Weddell Sea if (i) the SIE time series of the observations falls below -1σ *and* the time series of the model is concurrently below -0.5σ or (ii) the SIE time series of the model falls below -1σ *and* the time series of the observations is concurrently below -0.5σ. We choose to focus on the JFM seasonal mean (see
130   climatology in Fig. S1) not only because the absolute minima can occur in both February (as in 2022, see Thompson, 2022) and March (as in 2017, see Turner et al., 2017), but also because the model is known to be biased towards excessive melting that results in little sea ice left in February (e.g. Vancoppenolle et al., 2012).

The anomalies are computed with respect to the climatology of the entire period (1980-2022). The statistical significance of the composites is assessed with bootstrapping by building 500 synthetic composites with the same number of years randomly
135   sampled from the same period. The threshold for significance is set to 90%.
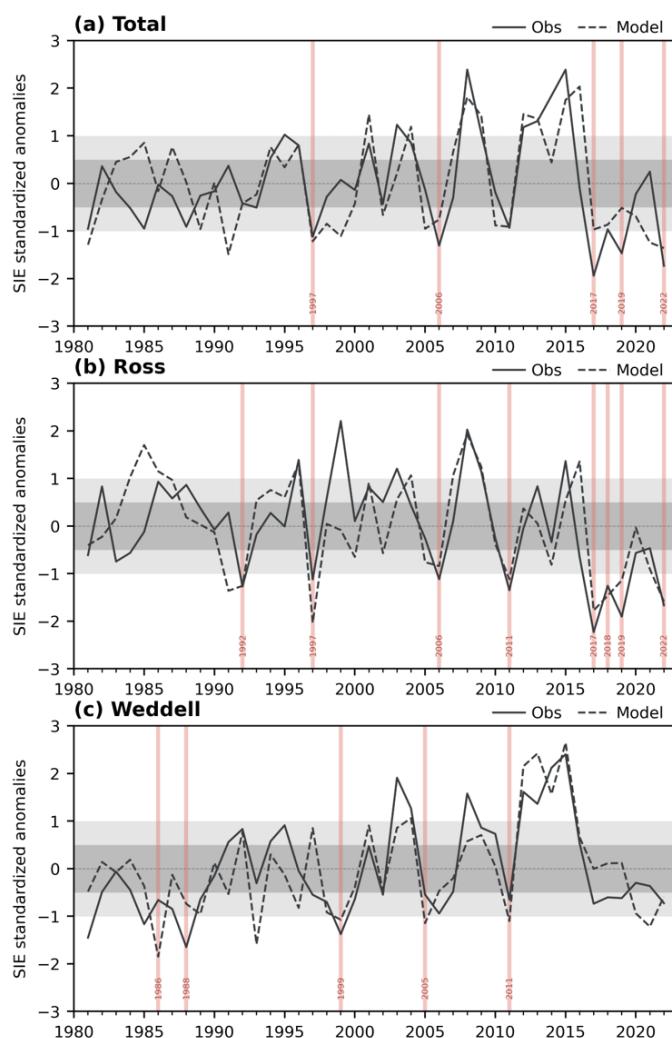
Figure 1: Standardized SIE anomalies in JFM computed over (a) the total SO domain (b) the Ross region (c) the Weddell region. Comparison between observations (solid line) and model (dashed line). Years with a minimum SIE are marked in red.

2.3 Sea ice concentration budget

140 In general terms, the temporal evolution of SIC at a certain location can be expressed as:

$$\frac{dSIC}{dt} = dyn + thermo$$

where *dSIC/dt* is the SIC tendency and *dyn* and *thermo* are dynamic and thermodynamic terms, respectively, whose exact definitions can vary. Typically, the dynamic term encapsulates the effect of ice motion, namely advection and divergence, while the thermodynamic term represents local ice melting and formation. In Sect. 3.5, we evaluate this budget with a model

145 diagnostic that, at each time step, splits the total grid-point SIC tendency into a dynamic term that includes advection and divergence but also mechanical redistributions (such as ridging and rafting), and a thermodynamic term. The thermodynamic contribution is mainly dominated by melting and formation of new ice in open water, but is also influenced by vertical processes such as bottom growth, bottom melt, surface melt and snow ice formation (e.g. Barthélemy et al., 2018).

A similar tool developed for observations by Holland and Kwok (2012) uses slightly different definitions. The SIC tendency

150 is computed explicitly as the difference between successive time steps. The dynamic term corresponds to the sum of SIC advection and divergence, which are computed directly using observed sea ice motion vectors. Then, the difference between these two terms is a residual that is attributed to thermodynamics and other secondary processes, including redistribution mechanisms. While this diagnostic was used in successive works to analyze climatologies and trends, and even applied to numerical model outputs (e.g. Lecomte et al., 2016; Holmes et al. 2019), it relies on sea ice motion observations that are not

155 always available and reliable, particularly for the melting season. To analyze anomalies in our small sample of summer events, we thus preferred to use the model diagnostics, which are computed online during the simulation, even though they may be affected by the model's biases.

3 Results

3.1 Sea ice extent time series and selection of events

160 Examining the temporal evolution of the summer SIE anomalies (Fig. 1), an overall good agreement between the model and the observations is found, with a correlation between the time series of 0.65, even though the model appears to perform worse during the first 10-15 years. According to the criteria described in Sect. 2.3, five years with minimum total SIE are selected (Fig. 1a). These five years (1997, 2006, 2017, 2019, 2022) all fall in the range of the last two thirds of the examined period, which could be partly linked to the increased variability over the recent years that is evident in Fig. 1. Additionally, several

165 years can be identified as regional minima in the Ross and Weddell sectors, based on their respective SIE time series (Fig. 1b,c). All the years identified as total minima are also minima in the Ross Sea, but none of them is a minimum in the Weddell Sea, indicating different contributions from these two regions to the total minima. Additionally, three years that are exclusively

regional minima are detected for the Ross sector (1992, 2011 and 2018) and five for the Weddell sector (1986, 1988, 1999, 2005, 2011), with only one common year (2011).

3.2 Sea ice concentration

The related maps of observed JFM SIC anomalies during the five total minima and their composite are shown in Fig. 2. Negative anomalies, indicating an unusually low SIC, are mostly present in the Ross and Weddell sectors in all years, yielding a robust and significant signal in the composite map (Fig. 2f). However, the amplitude and location of the anomalies show some variability in both regions. In the Ross Sea, the negative anomalies in the three most recent years (Fig. 2c,d,e) are located near the coast and extend to most regions from 180 to 120°W, with values exceeding -0.5. In contrast, the remaining two years show a more complex structure, with mixed positive and negative anomalies (Fig. 2a,b). A more consistent signal is found in the Weddell Sea, with dipole-like anomalies that show an anomalous increase in SIC near the continent, and an anomalous decrease at the sea ice edge over almost the entire sector; only 2022 stands out for the more westward location of the negative anomalies.
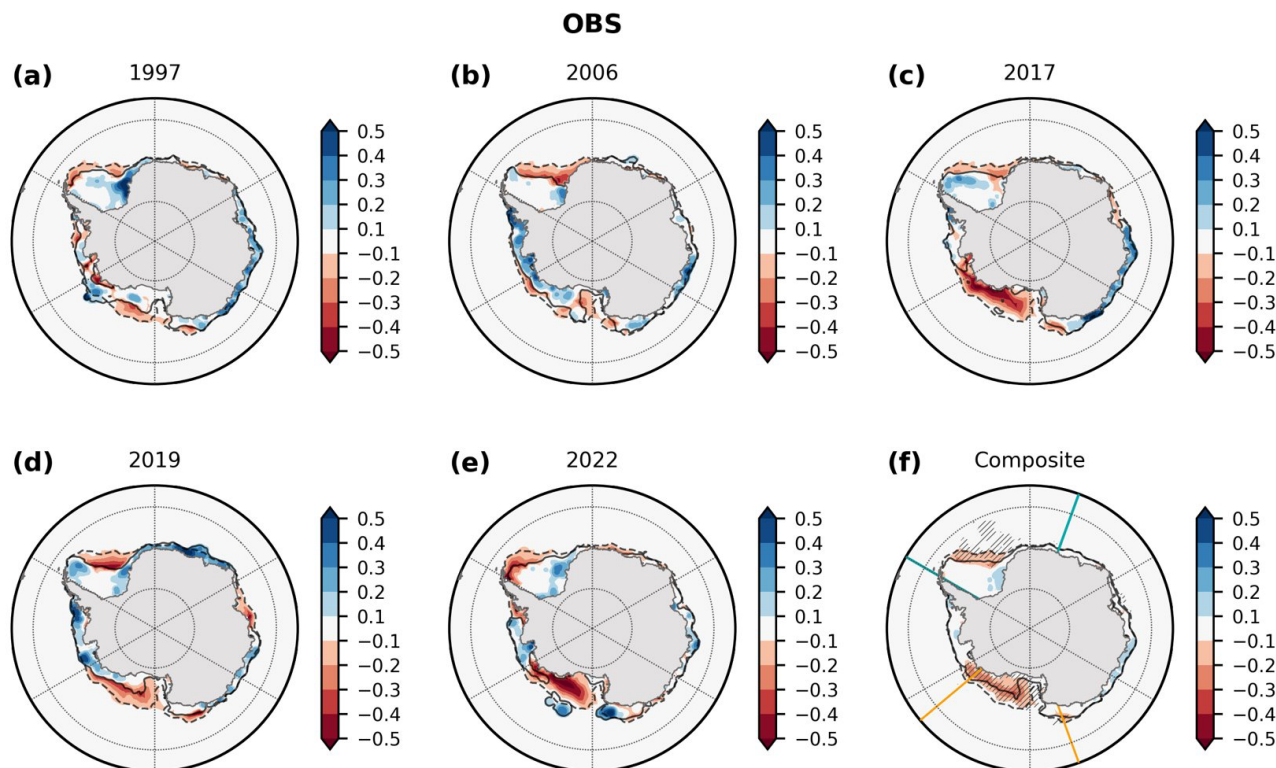
Figure 2: Shading: observed SIC anomalies in JFM in the years with total SIE minima (panels a-e) and their composite (panel f). Contours: sea ice edge (SIC=0.15) in the respective years (solid line) and in the climatology (dashed line). Hatching in the composite map indicates statistically significant values, while the orange and green lines show the boundaries of the Ross and Weddell sectors, respectively.

In the model, negative anomalies dominate in the Ross Sea and extend through the entire sector in 1997, 2017 and 2022 (Fig.

185 3a,c,d), while positive anomalies are also present in the region in 2006 and 2019. The resulting signal in the composite is a negative anomaly peaking west of 180°, in contrast with the observations, which tend to peak east of the dateline (cf. Fig. 3f and 2f). This difference may be related to model biases in the summer climatology (see Fig. S1). While the positive signal in the Weddell Sea that is evident in the observations is also reproduced by the model, only sparse negative anomalies are found in the model in the single years (Fig. 3a-d) and are almost lacking in the composite map (Fig. 3f). Note that the model

190 systematically underestimates the SIE in summer, which may explain the lack of negative anomalies in the Weddell Sea and the different anomalous pattern in the Ross Sea (see Fig. S1). The model also seems to fail in reproducing well the strength of the anomalies, particularly for the 2017 and 2022 events. This may be also due to systematic biases in the model's mean state, which can affect the simulation of the anomalies: for example, a too thick baseline mean sea ice state in the model could explain that the summer sea ice area anomalies in a warm year are not as large as the observed ones.
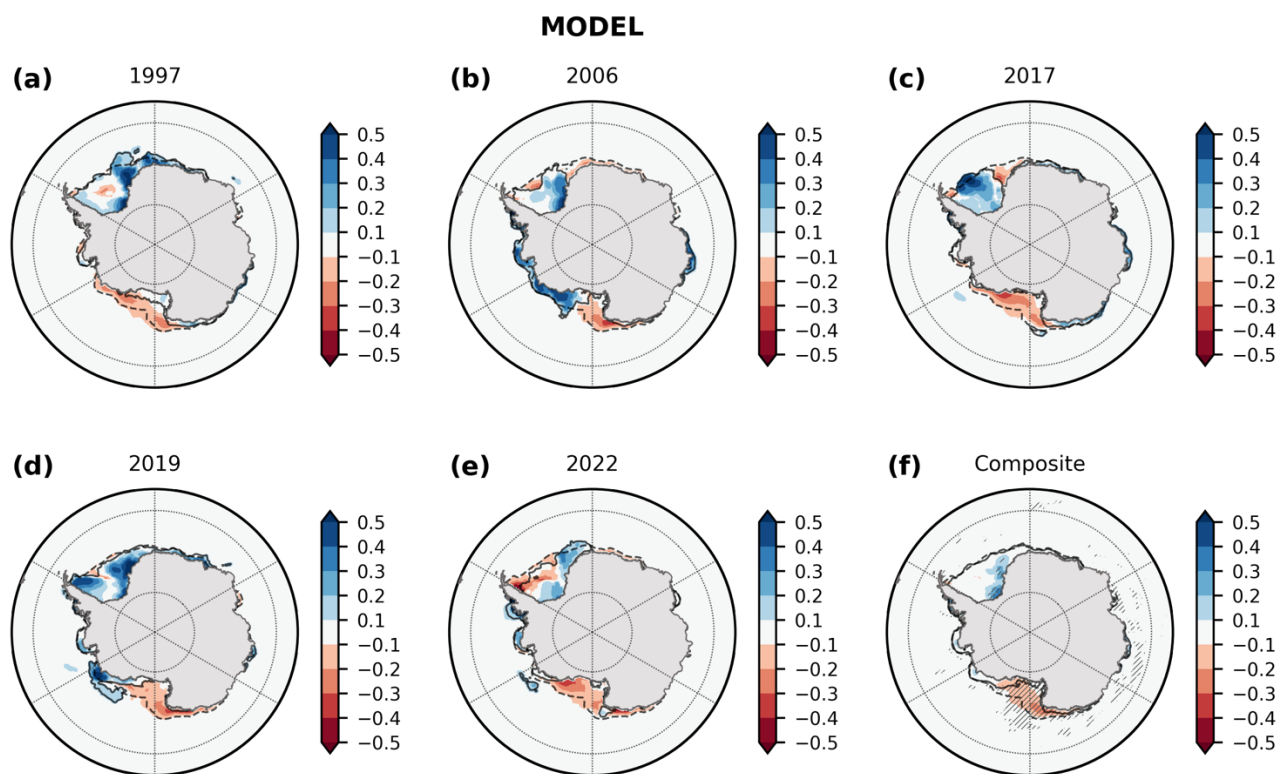
195

Figure 3: Same as Fig. 2, but for the model.

Interestingly, years that are minima exclusively in the Weddell Sea show strong negative anomalies in the observations in that region, similar to the total case, but mostly positive ones in the Ross Sea, again confirming that the two sectors do not always

200 contribute simultaneously to a total minimum (see Fig. S4). In contrast, turning to the Ross Sea regional minima, 1992 shows

a similar pattern with anomalies of opposite sign in the two regions, while 2018 displays negative anomalies in both of them (Fig. S2). The year 2011, which is a regional minimum for both sectors, expectedly features a mixed signal (Fig. S2): as it can be noted in the time series, it is very close to being defined as a total minimum (Fig. 1a), but positive anomalies in the Amundsen and East Antarctic sectors partially compensate for the negative ones in the Ross and Weddell Seas. Though with
205 different patterns and amplitudes, roughly similar results are found in the model (Figs. S3 and S5), except for 2005, that is a regional minimum in the Weddell Sea with pronounced negative anomalies in both sectors.

Overall, it emerges that the Weddell and Ross Seas are the main regions contributing to the summer minima. Specifically, the Ross Sea's contribution to the total SIE anomalies (as in Fig. 1a) is about twice the one from the Weddell Sea in the observations (Table 1): on average, the Ross Sea accounts for around 105% of the negative SIE anomalies, and the Weddell
210 Sea for around 49% (note that their sum exceeds 100% as other sectors contribute with positive anomalies). In the model, the Ross Sea's role is even larger (around 160%), while the Weddell Sea's contribution is highly variable and typically underestimated. While the predominant role of these two regions is partly expected from the climatological distribution of sea ice, which tends to disappear in the other sectors during summer, it is interesting to notice that the signal is clear and robust also in the composites. However, the two sectors appear to behave independently, sometimes being even anti-correlated, with
215 regional minima corresponding to regional high SIE in the other sector. In general, the Ross Sea shows a larger variability and a higher number of recorded minima, which often correspond to total ones. Furthermore, anomalies in the Weddell Sea tend to show a dipolar distribution with increased SIC next to the continent and decreased SIC at the sea ice margin. This pattern is not always captured by the model, which underestimates the climatological summer extent, but there is overall good agreement between the model and observations. The model thus proves to be a valid tool to investigate the processes at play that cannot
220 be diagnosed from observed fields (Sect. 3.5).

Year		Total	Ross	Weddell
1997	Observations	-1.121	-1.122 (100.1%)	-0.550 (49.1%)
	Model	-1.217	-2.033 (167.0%)	+0.851 (-69.9%)
2006	Observations	-1.308	-1.119 (85.5%)	-0.943 (72.1 %)
	Model	-0.760	-0.843 (110.9 %)	-0.468 (61.6 %)
2017	Observations	-1.942	-2.230 (114.8 %)	-0.737 (37.9 %)
	Model	-0.971	-1.775 (182.9 %)	-0.005 (0.6 %)
2019	Observations	-1.470	-1.904 (129.5 %)	-0.620 (42.2 %)
	Model	-0.517	-1.142 (220.9 %)	+0.117 (-22.6 %)
2022	Observations	-1.733	-1.665 (96.1 %)	-0.726 (41.9 %)
	Model	-1.361	-1.586 (116.5 %)	-0.586 (43.1 %)

Table 1: Standardized SIE anomalies in JFM (as in Fig. 1) during the years selected as circumpolar minima in the observations and model. The values refer to the SIE computed over the entire Southern Ocean domain (Total) and over the Ross and Weddell sectors in the respective columns. The percentages in parenthesis indicate the relative contribution of the two sectors to the total (negative) anomalies. Note that, for
225 a certain year, the sum of the two percentages can exceed 100% due to the positive contributions from other sectors.

3.3 Role of winter sea ice extent

So far, we have focused on summer and based our definition of the minima on SIE anomalies in JFM, since this season also corresponds to the minimum in the climatological seasonal cycle of sea ice extent. However, one may wonder whether these summer minima are preceded by anomalous sea ice conditions during the previous seasons. In particular, negative SIE
230 anomalies already in winter would correspond to less sea ice to melt during the following months and could hence favor the summer minima.

To explore this hypothesis, we considered monthly standardized SIE anomalies ranging from the preceding September, i.e. when the annual maximum is reached at the end of winter, to March. In the observations, negative anomalies of the total SIE extent (Fig. 4a) start to appear already in September and are maintained until March for the last three years (2017, 2019 and
235 2022), while 1997 displays a mixed behavior and 2006 only shows signs of an incoming minimum from December onwards. This may suggest a role of winter preconditioning at least during the most recent years, but the model is not able to reproduce this behavior, since clear negative anomalies during all six months are seen in 2022 only (Fig. 3d). The results for the regional minima in the Weddell and Ross sectors (Fig. 3, center and bottom columns) also do not support a straightforward link between winter and summer anomalies. In contrast to the total SIE, the results are very similar in the model and the observations for
240 each region. Some years show indeed consistent negative anomalies through most of the warm season (1992, 2018, 2019 in the Ross Sea; 1999 and 2011 in the Weddell Sea), so that the influence of the winter sea ice state cannot be excluded, but it is not the case in many other years and the preconditioning of a summer minimum by reduced winter extent seems to be marginal.
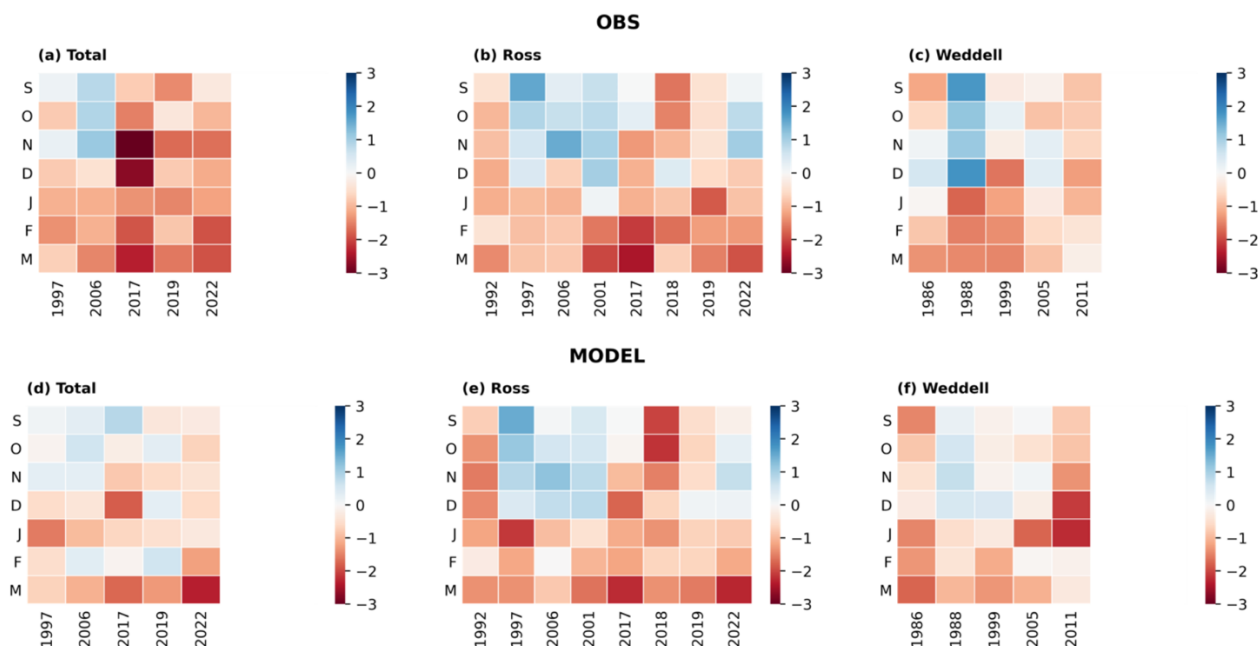
Figure 4: Monthly standardized SIE anomalies in the observations (top) and model (bottom) for the years with summer SIE minima, starting
245 from the previous September. SIE computed over (a) the total SO domain (b) the Ross region (c) the Weddell region.

3.4 Atmospheric circulation and surface winds

Different processes may contribute to the anomalous melting of sea ice resulting in a SIE minimum. Since winds strongly influence sea ice through both heat advection and mechanical transport, anomalous conditions in the atmospheric circulation during the preceding months could drive the summer SIE events (Holland and Kwok, 2012; Hobbs et al., 2016; Kusahara et al., 2019). Hence, in this section, we examine sea-level pressure (SLP) and 10m-wind anomalies during the previous season, OND, that lead to minimum sea ice extent in summer. The importance of atmospheric spring conditions for the summer and autumn sea ice state has been shown in several studies (e.g. Holland et al., 2017; 2018), and previous works examining the 2017 and 2022 minima also considered this season (e.g. Purich and England 2019; Yadav et al. 2022). Furthermore, as seen in the previous section, the sea ice anomalous conditions are already set up in January at the latest, indicating the important role of surface winds during the previous months.

Anomalous maps of SLP and winds for the total minima are shown in Fig. 5 (similarly to Fig. 1 and 2): note that they are the same for the reanalysis and the model, since the latter is forced by the same atmospheric fields (see Sect. 2). The ASL seems to play a role, since anomalous SLP centers are present in the Bellingshausen-Amundsen sector during most years. However, the ASL is sometimes strengthened (1997, 2022; Fig. 5a,e) and sometimes weakened (2006, 2017; Fig. 5b,c). A deepened ASL emerges in the composite (Fig. 5f), but this signal is likely dominated by 2022, which shows strong anomalies beyond –10 hPa (Fig. 5e). Mixed conditions also emerge for the SAM, with some years characterized by more westerly winds (1997, 2019, 2022) and others in which the westerly winds seem weaker. Similarly, the corresponding patterns for the regional minima in the Weddell and Ross sectors are quite diverse and do not provide a clear indication of a preferred status of the ASL or other large-scale features in the months prior to a SIE summer minimum (Figs. S6 and S7).

Even if they might emerge from different large-scale patterns, the anomalous low-level winds exhibit at least a dominant direction in the two key sectors (Ross and Weddell) for most of the years, which roughly corresponds to the direction appearing in the composite. We confirm and quantify this by computing the average wind direction in the Weddell and Ross sectors (as defined in Sec. 2.2) over the grid points with negative JFM SIC anomalies greater than –0.1 (namely, areas with red shading in Figs. 2 and 3). Note that, in this case, different values for the observations and model are shown, since the SIC anomalies are distinct. The results for all the years, including total and regional minima, are reported in Fig. 6 in terms of wind angle with respect to the zonal direction: an angle of 0° (180°) represents pure westerly (easterly) winds and a value of 90° (270°) indicates a pure southerly (northerly) component. Most points are found in the first and fourth quadrants, indicating that the anomalous winds during these years are predominantly westerly, but have varying meridional components. In the Ross region (orange points) the values are confined to a small range, being mostly found between around 310° and 60°, which suggest a prevailing westerly/south-westerly component. In contrast, a larger spread is observed concerning the Weddell sector (green points), but approximately two thirds of the points are found in the fourth quadrant, indicating a dominant north-westerly component. A notable exception is 2017, particularly in the observations, with a mostly southerly component in the Weddell Sea, as seen in Fig. 5c.

Though it is challenging to identify common large-scale circulation anomalies, and hence to highlight a systematic influence
280   of drivers such as the El Niño-Southern Oscillation (ENSO) or the SAM, we have shown that the regional wind conditions in
the Ross and Weddell sectors share some similarities across the minima. The dominant north-westerly anomalous winds in the
Weddell Sea are consistent with the dipolar distribution of SIC, with warm air incoming from lower latitudes that pushes the
sea ice towards the coasts of Antarctica (Figs. 1f,2f and 4f). The prevailing south-westerly anomalous flow in the Ross Sea, in
contrast, suggests winds mainly coming from the continent and transporting the sea ice away. The exact roles of ice transport
285   and thermodynamic melting in leading to the summer SIC anomalies are examined in detail in the next section, for both
regions.
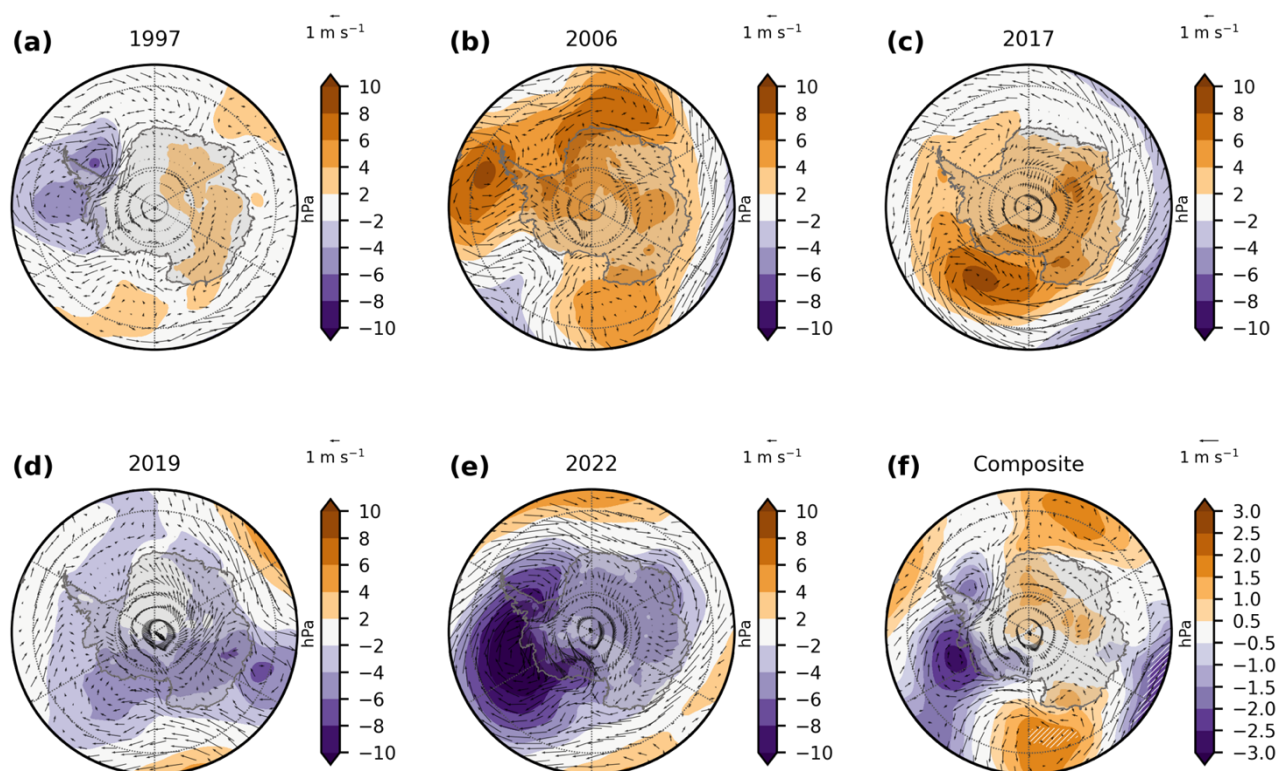
290   **Figure 5:** SLP (shading) and 10-m wind (arrows) anomalies in the years with total SIE minima (panels a-e) and their composite (panel f)
during the previous spring (OND). Hatching in the composite map indicates statistically significant SLP values.
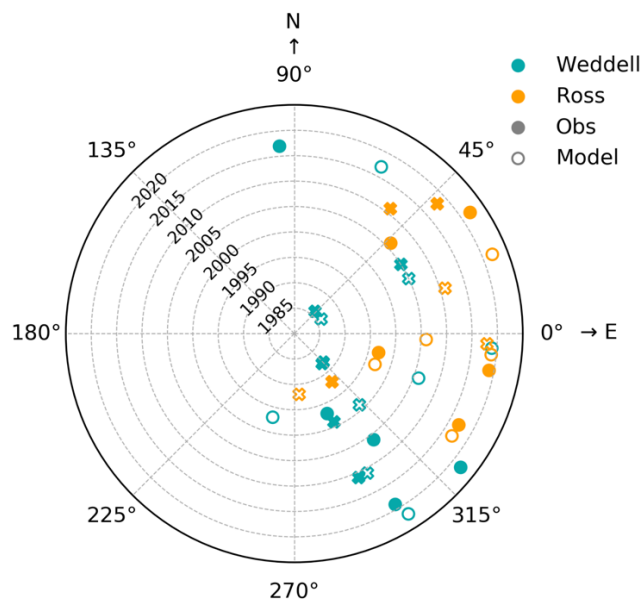
Figure 6: Average OND 10-m wind direction (angle with respect to zonal axis) for all extreme years in the observations (full circles) and model (empty circles). See main text for details.

3.5 Sea ice concentration budget

We have shown that the exceptional sea ice melting during the minima appears to be related to anomalous surface winds that share some common regional features throughout most of the events. However, the fundamental mechanisms governing this exceptional reduction have not been examined yet, and, in particular, the contribution of dynamic and thermodynamic processes. To assess this, we used the model diagnostics for the SIC budget described in Sect. 2.3. We computed the anomalous values of the dynamic and thermodynamic terms for the minima over November-January (NDJ), to encompass the sea ice evolution during the two seasons examined above (OND and JFM) but focusing on the melting season for consistent anomalies (see the monthly climatologies in Figs. S8-10). Then, the values were averaged over areas in the Weddell and Ross sectors with negative JFM SIC anomalies (< -0.1), similarly to Fig. 6. The results reported in Fig. 7 thus represent the mean relative contribution of the dynamic and thermodynamic components to the total SIC change in the two regions, for all years (total and regional minima). In both sectors, most years present negative values for the two terms, indicating that both type of processes tend to lead to direct sea ice loss, for instance due to surface winds advecting warm air towards a region, thus favoring melting, while transporting sea ice away from it. In few years, such as 1997 in the Ross Sea (top), 2017 in the Weddell Sea (bottom), and 2007 in both regions, a moderate positive contribution from the dynamics is present, suggesting that more sea ice is transported mechanically to the area only for it to rapidly melt (negative thermodynamic term), again yielding an overall negative anomalous tendency. The prevailing southerly wind direction in the Weddell sector in 2017 is indeed different than

315   the rest of the years (see Fig. 6) and consistent with exceptional ice convergence and melting in the north-eastern part of the basin (cf. Figs. 3c and 4c).

The thermodynamic term typically exceeds, in absolute value, its dynamic counterpart, suggesting a predominant but not exclusive role of thermodynamics over dynamics. Some notable exceptions are however present: in 2022, dynamics seems to lead in both sectors, as in 2011 and 2017 in the Weddell region, though sometimes with only a small difference. The

320   thermodynamic term is mostly negative and its range is similar in the two sectors: from -1.317 to -0.140 $\times 10^{-3}$ day^{-1} in the Ross Sea and between -1.143 to 0.066 $\times 10^{-3}$ day^{-1} in the Weddell Sea. In contrast, the dynamic term spans both positive and negative values, between -0.558 and 0.336 $\times 10^{-3}$ day^{-1} in the Ross Sea and ranging from -1.908 to 1.168 $\times 10^{-3}$ day^{-1} in the Weddell Sea, confirming that the two terms can be comparable in some cases, particularly in the Weddell sector.
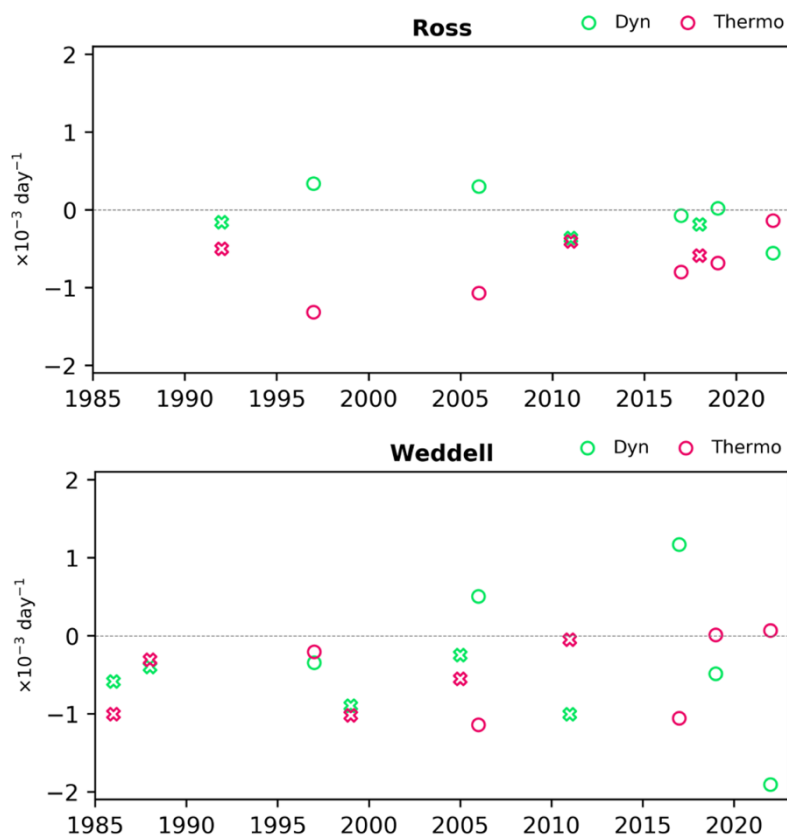
325

Figure 7: Average anomalous dynamic (green) and thermodynamic (magenta) contributions to the sea ice budget in NDJ for the (a) Ross and (b) Weddell regions. See main text for details.

4 Discussion and conclusions

330   We have examined sea ice and atmospheric conditions before and during summer SIE minima over the satellite period, in observations and in a regional ocean-sea ice model driven by atmospheric fields from ERA5. We have highlighted that the sectors mainly contributing to circumpolar minima are the Weddell and Ross seas, in agreement with previous studies for 2017 (e.g. Turner et al., 2017) and 2022 (e.g. Wang et al., 2022) and consistent with the summer climatological conditions, which feature little sea ice in the other sectors. However, we have also highlighted regional differences: the Ross Sea experiences a

335   higher number of recorded minima, which often correspond to total ones; in turn, regional minima in the Weddell Sea are usually balanced by excess of sea ice in the other sectors. Hence, the variability of the Ross Sea seems to lead the minima, even though the synergy with the Weddell Sea was crucial in the latest cases (2017, 2019, 2022). These results are consistent with previous reports of strong regional differences in the inter-annual and long-term variability of Antarctic sea ice (e.g. Zwally et al., 2022; Parkinson and Cavalieri, 2012; Comiso et al., 2017) but are here applied to SIE minima for the first time.

340   We have also shown that, during these events, SIC anomalies in the Weddell Sea tend to present a dipolar distribution, with anomalous ice accumulation towards the continent, while the Ross Sea tends to have a more homogenous decrease. This further stresses the regional differences and suggests distinct mechanisms at play in the two sectors. To investigate these mechanisms, we have tested various processes potentially contributing to the development of the summer SIE minima: the role of wintertime sea ice conditions prior to the minima, the impact of the anomalous springtime winds, and the contribution of dynamics and

345   thermodynamics to the exceptional sea ice loss.

First, we have explored the hypothesis that the summer minima are preceded by anomalous sea ice conditions already in winter and are hence a consequence of less sea ice being available for melting in the first place. However, by examining monthly SIE anomalies from the previous September, we have not found a clear and consistent role of the wintertime sea ice preconditioning. In fact, this contribution seems to be minor in most years before 2017, indicating that those minima are mainly

350   driven by atmospheric conditions. However, a more prominent role emerges for the last events (2017, 2019, 2022); more data from the next years are needed to understand if it is accidental or if new patterns are emerging.

Next, considering the prominent impact of winds on sea ice variability (Holland and Kwok, 2012; Hobbs et al., 2016; Kusahara et al., 2019), we have examined the role of surface atmospheric circulation anomalies during the previous spring in driving the summer SIE minima. Surface winds, and hence sea ice, can be modulated by typical modes of atmospheric variability such as

355   ENSO, the SAM, the ZW3 pattern, the Indian Ocean Dipole and other remote forcings, for instance from the stratosphere (e.g. Turner, 2004; Raphael, 2007; Thompson et al., 2005). In particular, the 2022 minima has been attributed to the combined effects of La Niña and a positive SAM, which both contributed to strengthening the ASL (e.g. Turner et al., 2022). Here, we have not explicitly examined these modes of variability, but by visual inspection of the SLP anomalies over the Southern Ocean in OND, we have not recognized consistent atmospheric patterns through the different minima that can be related to

360   their atmospheric signatures. Hence, our analysis does not identify a clear unique large-scale atmospheric mode as the driver of the summer SIE minima, though we acknowledge the potential impact of the superposition of different modes. More

generally, there is not a clear anomalous atmospheric pattern emerging as a common feature to all or most minima, such as a preferred status of the ASL. Instead, the large-scale circulation seems to be more related to the specific events, with anomalous SLP centers of action in distinct locations depending on the case. However, we argue that different large-scale anomalies in the atmospheric circulation can nonetheless lead to similar regional prevailing winds, which ultimately influence the sea ice variability. Specifically, our results indicate that SIE minima are associated with dominant north-westerly anomalous winds in the Weddell Sea and a prevailing south-westerly anomalous flow in the Ross Sea. These local atmospheric conditions seem to be the main common driver to most summer SIE extremes.

Finally, we investigated whether the anomalous sea ice loss leading to a summer SIE minimum is mostly driven by dynamic processes, such as sea ice motion and mechanical redistribution, or thermodynamic contributions, such as the melting of sea ice in open water or local vertical processes. The regional differences concerning the predominant winds could suggest distinct contributions from dynamics and thermodynamics in the Ross and Weddell Seas; however, our results are similar for the two regions. We find that the exceptional sea ice loss in both sectors is generally dominated by thermodynamic processes, though dynamics also play a role, but minor. These results are consistent with Wang J. et al. (2022)'s estimate for the 2022 event, for which they found that both terms contribute in spring to the anomalous sea ice loss, and with Kusahara et al. (2018), who demonstrated the prevalence of thermodynamic forcings for the spring extreme in 2016, ahead of the summer 2017 minimum. Both types of contributions are influenced by the winds, which transport warm and cold air masses as well as the sea ice itself, but also by other processes. Note that the thermodynamic and dynamic terms have to be interpreted carefully, as these processes are not strictly separated. For instance, sea ice transport can create leads that induce a warming and melting associated with the albedo-temperature feedback (e.g. Goosse et al. 2023), but this melting would be accounted for in the thermodynamic part in the framework proposed here.

Note that several alternative selection criteria for the minima could be used. For instance, Turner et al. (2019) simply considered the lower quartile of sea ice annual minimum extents. The method does not strongly affect the final collection of years in the observations, where the total minima could be identified almost by eye (Fig. 1a), but in our case it is relevant for the comparison with the model. We selected the events based on concurrent conditions for both the observed and modelled time series to ensure the analysis of a reasonable number of observed events that are also captured by the model.

We finally remark that the model's results must be interpreted within the simulation biases and limitations. For instance, the experimental set up with imposed atmospheric conditions does not permit to estimate the influence of the ocean-sea ice system on the atmosphere, and consequent feedbacks, which likely play a role in the occurrence of minima (e.g. Goosse et al. 2023). Furthermore, not only is the model's summer climatology biased towards too low extent, as discussed above, but it also tends to underestimate the SIC anomalies during all months. Nevertheless, the model's results are consistent with the observations and with previous works and support our conclusions.

As we prepare this paper, at the beginning of 2023, Antarctic sea ice has not recovered from last year's minimum, maintaining anomalously low values during and after the growing season. It is probable that a new record will be established, raising more

395 concerns about the future of Antarctic climate. With this work, we contribute to understanding the main process of driving these extreme events as we wait for the likely next record to see how it will fit with our conclusions

Code and data availability

The OSI-SAF data are available at https://osi-saf.eumetsat.int/products/osi-450 (1979-2015) and https://osi-saf.eumetsat.int/products/osi-430-b-complementing-osi-450 (2015 onwards). The ERA5 data can be downloaded from the
400 Copernicus Climate Data Store: https://cds.climate.copernicus.eu/cdsapp#!/dataset/reanalysis-era5-single-levels-monthly-means?tab=overview. The NEMO3.6 version is available from https://forge.ipsl.jussieu.fr /nemo/browser/branches/UKMO (Mathiot and Storkey, 2018).

Acknowledgements

This work was performed in the framework of the PARAMOUR project, "Decadal predictability and variability of polar
405 climate: the role of atmosphere-ocean-cryosphere multiscale interactions", supported by the Fonds de la Recherche Scientifique – FNRS – and the Research Foundation – Flanders (FWO) under the Excellence of Science (EOS) program (grant no. O0100718F, EOS ID no. 30454083). The computational resources were provided by the VSC (Flemish Supercomputer Center), funded by the FWO and the Government of Flanders; the Center for High Performance Computing and Mass Storage (CISM) of the Université catholique de Louvain (UCL); and the Consortium des Équipements de Calcul Intensif en Fédération
410 Wallonie-Bruxelles (CÉCI), funded by the Fonds de la Recherche Scientifique de Belgique (F.R.S.-FNRS) under convention 2.5020.11 and by the Walloon Region. Hugues Goosse is research director with the F.R.S.-FNRS. François Massonnet is a F.R.S.-FNRS research fellow.

References

Barthélemy, A., Goosse, H., Fichefet, T., and Lecomte, O.: On the sensitivity of Antarctic sea ice model biases to atmospheric
415   forcing uncertainties, Clim. Dyn., 51, 1585–1603, https://doi.org/10.1007/s00382-017-3972-7, 2018.

Goosse, H., Allende Contador, S., Bitz, C. M., Blanchard-Wrigglesworth, E., Eayrs, C., Fichefet, T., Himmich, K., Huot, P.-V., Klein, F., Marchi, S., Massonnet, F., Mezzina, B., Pelletier, C., Roach, L., Vancoppenolle, M., and van Lipzig, N. P. M.: Modulation of the seasonal cycle of the Antarctic sea ice extent by sea ice processes and feedbacks with the ocean and the atmosphere, The Cryosphere, 17, 407–425, https://doi.org/10.5194/tc-17-407-2023, 2023.

420 Hersbach, H., Bell, B., Berrisford, P., Hirahara, S., Horányi, A., Muñoz-Sabater, J., Nicolas, J., Peubey, C., Radu, R., Schepers, D., Simmons, A., Soci, C., Abdalla, S., Abellan, X., Balsamo, G., Bechtold, P., Biavati, G., Bidlot, J., Bonavita, M., De Chiara, G., Dahlgren, P., Dee, D., Diamantakis, M., Dragani, R., Flemming, J., Forbes, R., Fuentes, M., Geer, A.,

Haimberger, L., Healy, S., Hogan, R. J., Hólm, E., Janisková, M., Keeley, S., Laloyaux, P., Lopez, P., Lupu, C., Radnoti, G., de Rosnay, P., Rozum, I., Vamborg, F., Villaume, S., and Thépaut, J.-N.: The ERA5 global reanalysis, Q. J. Roy.
425   Meteor. Soc., 146, 1999–2049, https://doi.org/10.1002/qj.3803, 2020.

Hobbs, W. R., Massom, R., Stammerjohn, S., Reid, P., Williams, G., and Meier, W.: A review of recent changes in Southern Ocean sea ice, their drivers and forcings, Global Planet. Change, 143, 228–250, https://doi.org/10.1016/j.gloplacha.2016.06.008, 2016.

Holland, P. R. and Kwok, R.: Wind-driven trends in Antarctic sea-ice drift, Nat. Geosci., 5, 872–875,
430   https://doi.org/10.1038/ngeo1627, 2012.

Holland, M. M., Landrum, L., Raphael, M., and Stammerjohn, S.: Springtime winds drive Ross Sea ice variability and change in the following autumn, Nat. Commun., 8, 731, https://doi.org/10.1038/s41467-017-00820-0, 2017

Holland, M. M., Landrum, L., Raphael, M. N., and Kwok, R.: The regional, seasonal, and lagged influence of the Amundsen Sea Lowon Antarctic sea ice, Geophys. Res. Lett., 45, 11227–11234, https://doi.org/10.1029/2018gl080140, 2018.

435   Holmes, C. R., Holland, P. R., and Bracegirdle, T. J.: Compensating biases and a noteworthy success in the CMIP5 representation of Antarctic sea ice processes. Geophys. Res. Lett., 46, 4299–4307. https://doi.org/10.1029/2018GL081796, 2019.

Kusahara, K., Reid, P., Williams, G. D., Massom, R., and Hasumi, H.: An ocean-sea ice model study of the unprecedented Antarctic sea ice minimum in 2016, Environ. Res. Lett., 13, 84020, 2018.

440   Kusahara, K., Williams, G.D., Massom, R., Reid, P., and Hasumi, H.: Spatiotemporal dependence of Antarctic sea ice variability to dynamic and thermodynamic forcing: a coupled ocean–sea ice model study. Clim Dyn 52, 3791–3807, https://doi.org/10.1007/s00382-018-4348-3, 2019.

Lavergne, T., Sørensen, A. M., Kern, S., Tonboe, R., Notz, D., Aaboe, S., Bell, L., Dybkjær, G., Eastwood, S., Gabarro, C., Heygster, G., Killie, M. A., Brandt Kreiner, M., Lavelle, J., Saldo, R., Sandven, S., and Pedersen, L. T.: Version 2 of the
445   EUMETSAT OSI SAF and ESA CCI sea-ice concentration climate data records, The Cryosphere, 13, 49–78, https://doi.org/10.5194/tc-13-49-2019, 2019.

Lecomte, O., Goosse, H., Fichefet, T., Holland, P. R., Uotila, P., Zunz, V., and Kimura, N.: Impact of surface wind biases on the Antarctic sea ice concentration budget in climate models, Ocean Model., 105, 60–70, https://doi.org/10.1016/j.ocemod.2016.08.001, 2016.

450   Madec, G., Bourdallé-Badie, R., Bouttier, P.-A., Bricaud, C., Bruciaferri, D., Calvert, D., Chanut, J., Clementi, E., Coward, A., Delrosso, D., Ethé, C., Flavoni, S., Graham, T., Harle, J., Iovino, D., Lea, D., Lévy, C., Lovato, T., Martin, N., Masson, S., Mocavero, S., Paul, J., Rousset, C., Storkey, D., Storto, A., and Vancoppenolle, M.: NEMO ocean engine, Tech. rep., Insitut Pierre-Simon Laplace, Zenodo [code], https://doi.org/10.5281/zenodo.3248739, 2017.

Massonnet, F., Guemas, V., Fuckar, N. S., and Doblas-Reyes, F.J.: The 2014 high record of Antarctic sea ice extent, in:
455   Explaining extreme events of 2014 from a climate perspective, edited by: Herring, S. C., Hoerling, M. P., Kossin, J. P., Peterson, T. C., and Stott, P. A., B. Am. Meteorol. Soc., 96, 163–167, https://doi.org/10.1175/BAMS-D-15-00093.1, 2015.

Mathiot, P. and Storkey, D.: NEMO model code, MetOffice (UK) branch dev_isf_remapping_UKESM_GO6package_r9314, revision 11248, MetOffice [code], https://forge.ipsl.jussieu.fr/nemo/browser/branches/UKMO/dev_isf_remapping_UKESM_GO6package_r9314?rev=15667 (last access: 21 January 2022), 2018.

Meehl, G.A., Arblaster, J.M., Chung, C.T.Y., Holland, M. M., DuVivier, A., Thompson, L. A., Yang, D., and Bitz, C. M.: Sustained ocean changes contributed to sudden Antarctic sea ice retreat in late 2016, Nat. Commun., 10, 14, https://doi.org/10.1038/s41467-018-07865-9, 2019

OSI SAF: Global Sea Ice Concentration Climate Data Record v2.0 - Multimission, EUMETSAT SAF on Ocean and Sea Ice, http://dx.doi.org/10.15770/EUM_SAF_OSI_0008, 2017.

Pelletier, C., Fichefet, T., Goosse, H., Haubner, K., Helsen, S., Huot, P.-V., Kittel, C., Klein, F., Le clec'h, S., van Lipzig, N. P. M., Marchi, S., Massonnet, F., Mathiot, P., Moravveji, E., Moreno-Chamarro, E., Ortega, P., Pattyn, F., Souverijns, N., Van Achter, G., Vanden Broucke, S., Vanhulle, A., Verfaillie, D., and Zipf, L.: PARASO, a circum-Antarctic fully coupled ice-sheet–ocean–sea-ice–atmosphere–land model involving f.ETISh1.7, NEMO3.6, LIM3.6, COSMO5.0 and CLM4.5, Geosci. Model Dev., 15, 553–594, https://doi.org/10.5194/gmd-15-553-2022, 2022.

Parkinson, C. L. and Cavalieri, D. J.: Antarctic sea ice variability and trends, 1979–2010, The Cryosphere, 6, 871–880, https://doi.org/10.5194/tc-6-871-2012, 2012.

Parkinson, C. L.: A 40-y record reveals gradual Antarctic sea ice increases followed by decreases at rates far exceeding the rates seen in the Arctic, Proc. Nat. Acad. Sciences 116, 14414–14423, 10.1073/pnas.1906556116, 2019.

Purich, A. and England, M. H.: Tropical teleconnections to Antarctic sea ice during austral spring 2016 in coupled pacemaker experiments. Geophys. Res. Lett., 46, 6848–6858, https://doi.org/10.1029/2019GL082671, 2019.

Raphael, M. N.: The influence of atmospheric zonal wave three on Antarctic sea ice variability, J. Geophys. Res., 112, D12112, https://doi.org/10.1029/2006JD007852, 2007.

Raphael, M.N. and Handcock, M.S.: A new record minimum for Antarctic sea ice, Nat. Rev. Earth Environ., 3, 215–216, https://doi.org/10.1038/s43017-022-00281-0, 2022.

Raphael, M. N., and Hobbs, W.: The influence of the large-scale atmospheric circulation on Antarctic sea ice during ice advance and retreat seasons, Geophys. Res. Lett., 41, 5037-5045, https://doi.org/10.1002/2014GL060365, 2014.

Rousset, C., Vancoppenolle, M., Madec, G., Fichefet, T., Flavoni, S., Barthélemy, A., Benshila, R., Chanut, J., Levy, C., Masson, S., and Vivier, F.: The Louvain-La-Neuve sea ice model LIM3.6: global and regional capabilities, Geosci. Model Dev., 8, 2991–3005, https://doi.org/10.5194/gmd-8-2991-2015, 2015.

Schlosser, E., Haumann, F. A., and Raphael, M. N.: Atmospheric influences on the anomalous 2016 Antarctic sea ice decay, The Cryosphere, 12, 1103–1119, https://doi.org/10.5194/tc-12-1103-2018, 2018.

Simmonds, I. : Comparing and contrasting the behaviour of Arctic and Antarctic sea ice over the 35 year period 1979-2013, Ann. Glaciol., 56, 18-28, doi:10.3189/2015AoG69A909, 2015.

490 Stuecker, M. F., C. M. Bitz, and Armour, K. C.: Conditions leading to the unprecedented low Antarctic sea ice extent during the 2016 austral spring season, Geophys. Res. Lett., 44, 9008–9019, doi:10.1002/2017GL074691, 2017.

Thompson, D. W. J., Baldwin M. P., and Solomon, S.: Stratosphere-Troposphere Coupling in the Southern Hemisphere, J. Atmos. Sci., 62, 708-715, https://doi.org/10.1175/JAS-3321.1, 2015.

Thompson, T.: Antarctic sea ice hits lowest minimum on record , Nat. News, doi: https://doi.org/10.1038/d41586-022-00550-4, 2022.

495 Turner, J.: The El Niño-southern oscillation and Antarctica., Int. J. Climatol., 24,1-31, https://doi.org/10.1002/joc.965, 2004.

Turner, J., Phillips, T., Marshall, G. J., Hosking, J. S., Pope, J. O., Bracegirdle, T. J., and Deb, P.: Unprecedented springtime retreat of Antarctic sea ice in 2016, Geophys. Res. Lett., 44, 6868– 6875, doi:10.1002/2017GL073656, 2017.

Turner, J., Holmes, C., Caton Harrison, T., Phillips, T., Jena, B., Reeves-Francois, T., Fogt, R., Thomas, E. R., and Bajish, C.
500 C.: Record low Antarctic sea ice cover in February 2022. Geophysical Research Letters, 49, e2022GL098904, https://doi.org/10.1029/2022GL098904, 2022.

Vancoppenolle, M., Bouillon, S., Fichefet, T., Goosse, H. Lecomte, O., Morales Maqueda, M. A., and Madec, G.: LIM The Louvain-la-Neuve sea Ice Model, Tech. Rep. 31, Note du Pôle de Modélisation de l'Institut Pierre-Simon Laplace No. 31, ISSN No 1288-1619, available at: https://cmc.ipsl.fr/images/publications/scientific_notes/lim3_book.pdf (last access 21
505 January 2022), 2012.

Wang, G., Hendon, H.H., Arblaster, J.M., Lim, E.-P., Abhik, S., van Rensch, P.: Compounding tropical and stratospheric forcing of the record low Antarctic sea-ice in 2016, Nat. Commun., 10, 13, https://doi.org/10.1038/s41467-018-07689-7, 2019.

Wang, J., Luo, H., Yang, Q. Liu, J., Yu, L., Shi, Q., and Han, B.: An Unprecedented Record Low Antarctic Sea-ice Extent
510 during Austral Summer 2022.,Adv. Atmos. Sci., 39, 1591–1597, https://doi.org/10.1007/s00376-022-2087-1, 2022.

Yadav, J., Kumar, A., and Mohan, R.: Atmospheric precursors to the Antarctic sea ice record low in February 2022, Environ. Res. Commun., 4, 121005, 10.1088/2515-7620/aca5f2, 2022.

Zhang, L., Delworth, T.L., Yang, X., Zeng, F., Lu, F., Morioka, Y., Bushuk, M.: The relative role of the subsurface Southern Ocean in driving negative Antarctic Sea ice extent anomalies in 2016–2021, Commun Earth Environ, 3, 302,
515 https://doi.org/10.1038/s43247-022-00624-1, 2022.

Zuo, H., Balmaseda, M. A., Tietsche, S., Mogensen, K., and Mayer, M.: The ECMWF operational ensemble reanalysis– analysis system for ocean and sea ice: a description of the system and assessment, Ocean Sci., 15, 779–808, https://doi.org/10.5194/os-15-779-2019, 2019.

Zwally, H. J., Comiso, J. C., Parkinson, C. L., Cavalieri, D. J., and Gloersen, P.: Variability of Antarctic sea ice 1979–1998,
520 J. Geophys. Res., 107, doi:10.1029/2000JC000733, 2002.